Pergamon

Cement and Concrete Research 32 (2002) 357–362

CEMENT AND CONCRETE RESEARCH

# Hydration products of alkali-activated slag–red mud cementitious material

Zhihua Pan*, Lin Cheng, Yinong Lu, Nanru Yang

*College of Materials Science and Engineering, Nanjing University of Technology, No. 5 New Mofan Road, Nanjing 210009, China*

Received 10 May 2001; accepted 10 September 2001

**Abstract**

A new kind of alkali–slag–red mud cementitious material, abbreviated as ASRC, with both high early and ultimate strength and excellent resistance against chemical attacks has been developed by the application of composite solid alkali activator into slag–red mud mixture system. The hydration products of this cement at ambient temperature have been investigated by means of XRD, IR, TG-DTA, TEM, EDXA, etc. The results showed that the hardened cement paste was mostly consisted of C-S-H gel, being very low in Ca/Si ratio, very fine in size and extremely irregular in its shape. Neither $Ca(OH)_2$ and AFt, which are usually present in the hardened Portland cement paste, nor zeolite-like products have been detected. These characteristics are considered to be the chemical reasons for the high early and ultimate strength and good resistance against chemical attacks of the hardened ASRC cement paste. © 2002 Elsevier Science Ltd. All rights reserved.

*Keywords:* Alkali-activated cement; Hydration products; Granulated blast-furnace slag; Red mud; Cement

## 1. Introduction

The titled alkali–slag–red mud (ASRC) cement belongs to clinker free cementitious material, which is made from alkali activator, blast-furnace slag (BFS) and red mud in designed proportion. The similar cementitious material includes alkali-activated slag cement, alkali-activated phosphorous slag cement, alkali-activated slag–fly ash cement and alkali-activated slag–Pozzolan cement. The alkali-activated cementitious material was first investigated and invented by Glukhovsky [1] in 1950s. Research activities in this area were carried out later in France, America, Poland, etc. [2–4], and also carried out in China in 1980s [5–8]. So far, the characteristics of the alkali-activated cementitious material, such as high early and ultimate strength and excellent resistance to chemical attacks, have been recognized and paid a lot of interest by scholars in cement and concrete research area. However, the research activities so far were mostly concentrated on the alkali-activated cement compared with other similar systems. On other hand, the high price and shortage in supply of BFS as the main raw material of the alkali-activated slag cement formed an obstacle for the large-scale application in China. The attempt to use other industrial waste materials for the replacement of BFS to make low slag content alkali-activated cementitious materials, therefore, becomes an interesting and practical research topic in China. Meanwhile, the red mud discarded from alumina refining plant was almost remaining in nonrecycled state, except very little part for the replacement of clay in the manufacture of Portland cement. Gong [9] has reported that an ASRC cement was developed by using liquid water glass as an alkali activator and sodium phosphate as setting retarder. The author, on the base of the previous research, furthermore succeeded in the development of ASRC cement with both high early and ultimate strength and excellent resistance against chemical attacks by introduction of solid composite alkali activator into slag–red

Table 1
Chemical composition of slag and red mud used in experiments (%)

| Material | $SiO_2$ | $Al_2O_3$ | $Fe_2O_3$ | CaO | MgO | $TiO_2$ | $Na_2O$ | $K_2O$ | ig.loss | Σ |
|---|---|---|---|---|---|---|---|---|---|---|
| Slag | 33.80 | 14.14 | 1.22 | 42.82 | 5.42 | 0.34 | – | – | 0.44 | 98.78 |
| Red mud | 17.75 | 7.17 | 9.46 | 38.69 | 1.51 | 2.41 | 3.23 | 0.50 | 16.38 | 97.10 |

---

* Corresponding author. Tel.: +86-25-3316755-3209; fax: +86-25-3325463.

*E-mail addresses*: zhihpan@mail.njuct.edu.cn, zhihpan@public1.ptt.js.cn (Z. Pan).

PII: S0008-8846(01)00683-4

Table 2
Proportion of two ASRC cement specimens (%)

| No. | BFS | RM | NS[a] | NA[a] |
|---|---|---|---|---|
| S1 | 70 | 30 | 8 | 6 |
| S2 | 70 | 30 | 8 | – |

[a] Activators are measured in the base of total amount of slag and red mud.

mud mixture system instead of the liquid water glass and hereby investigated the hydraulic properties and the hydration products of the developed ASRC cement in detail [9–13]. The reasons contributing to the good performance of the so-called ASRC hardened cement paste have also been discussed in this paper.

## 2. Raw materials and test methods

### *2.1. Raw materials*

Red mud used was from Shan Dong alumina refining plant, with 0.080-mm sieve residue 4.0% and Blaine specific area 380 m$^2$/kg. Slag used in experiment is granulated BFS from Jinan steel refining plant, with 0.080-mm sieve residue 6.0% and Blaine specific area 355 m$^2$/kg. The chemical composition of slag and red mud is listed in Table 1. X-ray diffraction and electronic microscopy analysis showed that the slag was mostly comprised of vitrified phase, and the red mud (RM) contained amorphous silica aluminate phase and $\beta$-$C_2S$, $\alpha$-$Fe_2O_3$, calcite and $CaTiO_3$. The alkali activator is composed by solid water glass (NS) with modulus 1.2 and sodium aluminate clinker (NA), the 0.080-mm sieve residue being 5.0%.

### *2.2. Specimen preparation and testing conditions*

#### *2.2.1. Preparation of hydrated specimens*

Two kinds of ASRC cement used for preparation of hydrated specimens were selected, marked as S1 and S2. The proportions of S1 and S2 cements are listed in Table 2, with the S2 being composed of simple activator and S1 being made from composite activator.

Hydrated cement specimens were prepared in two ways, one being in the form of cement paste and another as a cement–water suspension. In the cement paste case, cement, both S1 and S2, was mixed with water in water/cement ratio 0.5, then cured in fog room at 20 ± 3 °C for 24 h, followed by curing in water at 20 ± 3 °C (abbre-

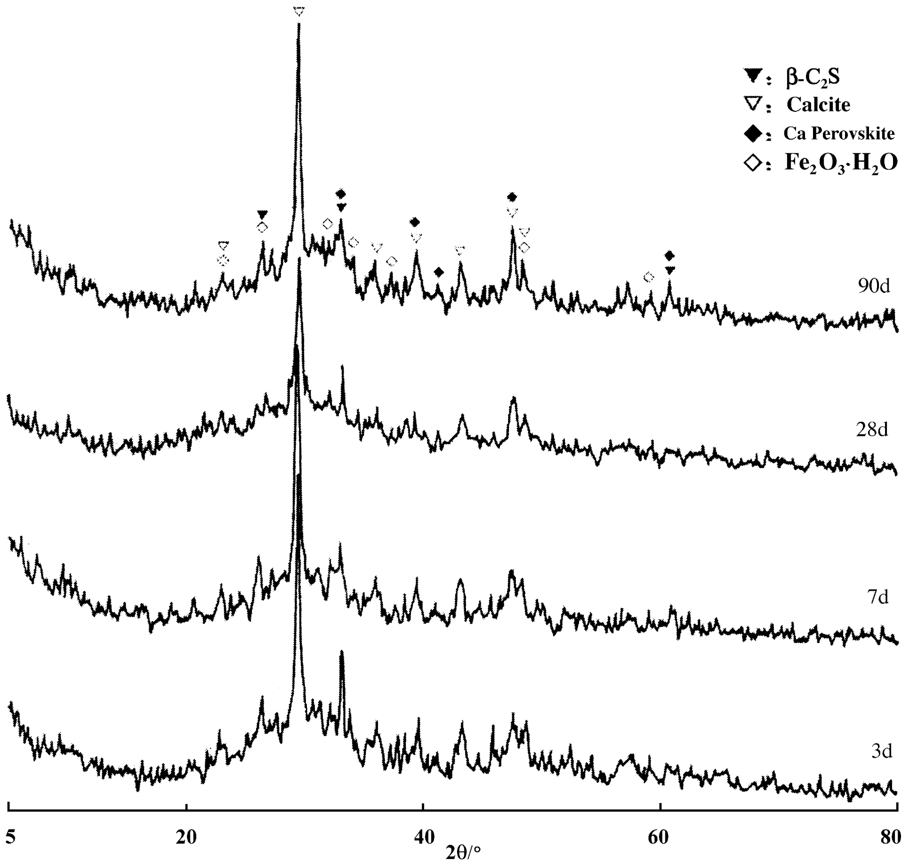

Fig. 1. XRD patterns of hydrated ASRC (S1) cement paste at different curing ages.

viated as ambient temperature curing below) and in steam at 80 °C (abbreviated as steam curing below). The hydration of cement paste was stopped by drenching in alcohol at the prescribed curing ages, followed by XRD, IR and TG-DTA analyses after grinding and drying.

For S1 cement, a suspension specimen with water/cement ratio 20 was prepared and cured at 20 ± 3 °C for 28 days. The dispersed hydration products were then observed under TEM and the compositions of the selected hydration product particles were analyzed by EDXA.

### *2.2.2. Testing conditions*

1. XRD analysis was conducted on the D/max-rB X-ray diffraction meter in powder diffraction method, with Cu *K*α, voltage 40 kV and current 100 mA.
2. TG-DTA analysis was carried out on WCT-2 differential thermal analyzer at heating rate 10 °C/min, from ambient temperature to 970 °C.
3. IR analysis was carried out on IR-75 infrared analyzer. KBr method was used.
4. TEM-EDXA analysis was carried out on H-800 analysis electronic microscope for morphology observation and on Analyst-8000 energy spectroscopy for composition analysis.

## 3. Results and discussion

### *3.1. Results of XRD analysis*

Figs. 1 and 2 show the results of XRD analysis on the hardened S1 and S2 cement paste specimens cured in standard condition at 3, 7, 28 and 90 days, which at least revealed something as follows:

All the XRD patterns show the similar features — therefore, the similar composition and almost the same as that of red mud specimen regardless of the difference of curing age and type of activator [13], indicating that all the crystallized minerals in the hardened cement paste system come from red mud and no new crystallized hydration products formed.

The diffraction strength of the β-$C_2S$ decreases with the increase of the curing age of the cement paste, which is more remarkable in the case of S1 specimen than that of S2 specimen, indicating that the hydration rate of β-$C_2S$ from red mud was in some extent accelerated by the addition of composite activator. Therefore, it is reasonable to say that the composite activator is more effective than the simple alkali activator.

Some researchers have reported [8] that zeolite-like minerals were found in the hardened alkali–slag cement paste system. The XRD analysis in this research on the 80 °C

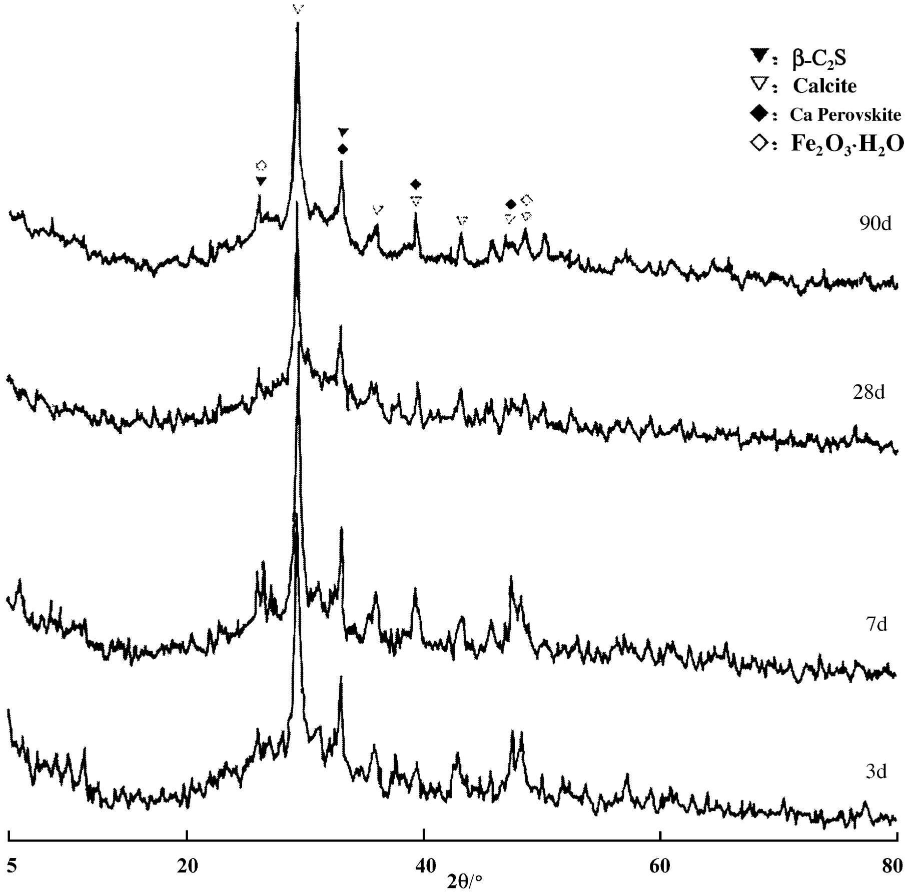

Fig. 2. XRD patterns of hydrated ASRC (S2) cement paste at different curing ages.

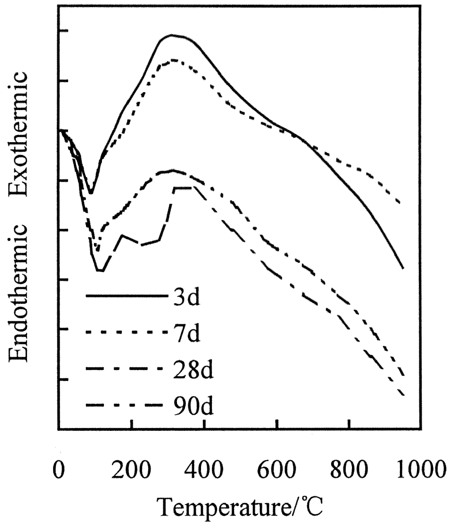

Fig. 3. DTA curves of hydrated ASRC (S1) cement paste at different curing ages during heating.

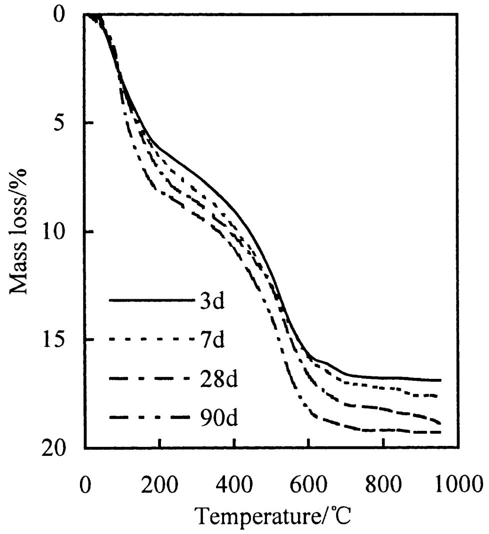

Fig. 4. Mass loss of hydrated ASRC (S1) cement paste at different curing ages during heating.

steam-cured S1 hardened cement paste specimen showed that no zeolite-like minerals were detected, from which it can be inferred that the formation of the zeolite-like minerals in hardened cement paste cured at ambient temperature is of very less possible.

### *3.2. Results of TG-DTA analysis*

Results of TG-DTA analysis on S1 hardened cement paste specimen cured at ambient temperature are shown in Figs. 3 and 4, which show the similar features as those of hardened Portland cement paste system except for the additional exothermic effect between 200 and 600 °C probably being caused by the oxidation from ferrous oxide to ferric oxide existed in red mud. The endothermic effect near 80 °C may be due to the discharge of absorbed water in capillary pores in the hardened cement paste. The floating of the base line of the DTA curves and the feature of continuous cascade mass loss imply the existence of large amount of C-S-H gel. Water in different bonding status in C-S-H gel structure has different bonding energy, thus has different temperatures of discharging and therefore result in the continuous cascade form of the mass loss curve. The discharging of water caused the decrease in density and the change of thermal conductivity of the cement paste specimen, therefore resulting the floating of the base line of the DTA curve.

It is appropriate to emphasize that no endothermic effect around 450 °C caused by the dehydration of $Ca(OH)_2$ was detected, which represents that no $Ca(OH)_2$ formed in

Table 3
Mass loss of hydrated ASRC cement pastes occurred in the different temperature ranges during heating (%)

| Temperature zone | | 20–200 °C | 200–450 °C | 450–650 °C | 650–950 °C | 450–950 °C | Total |
|---|---|---|---|---|---|---|---|
| S1 cured at room temperature | 3 days | 6.04 | 4.21 | 5.90 | 0.75 | 6.65 | 16.90 |
| | 7 days | 6.44 | 4.56 | 5.50 | 1.20 | 6.7 | 17.70 |
| | 28 days | 7.03 | 4.22 | 6.25 | 1.40 | 7.65 | 18.90 |
| | 90 days | 7.99 | 4.21 | 6.55 | 0.55 | 7.1 | 19.30 |
| S2 cured at room temperature | 3 days | 5.78 | 4.85 | 6.02 | 0.35 | 6.37 | 17.00 |
| | 7 days | 7.03 | 4.97 | 5.50 | 0.60 | 6.10 | 18.10 |
| | 28 days | 8.26 | 5.49 | 6.25 | 0.30 | 6.55 | 20.30 |
| | 90 days | 9.00 | 5.75 | 6.15 | 0.30 | 6.45 | 21.20 |
| S1 steam cured | 4 h | 3.98 | 4.37 | 5.85 | 0.50 | 6.35 | 14.70 |
| | 8 h | 4.70 | 4.64 | 5.66 | 1.70 | 7.36 | 16.70 |
| | 16 h | 5.82 | 4.58 | 6.10 | 1.50 | 7.60 | 18.00 |
| | 24 h | 7.17 | 4.33 | 6.50 | 2.00 | 8.50 | 20.00 |

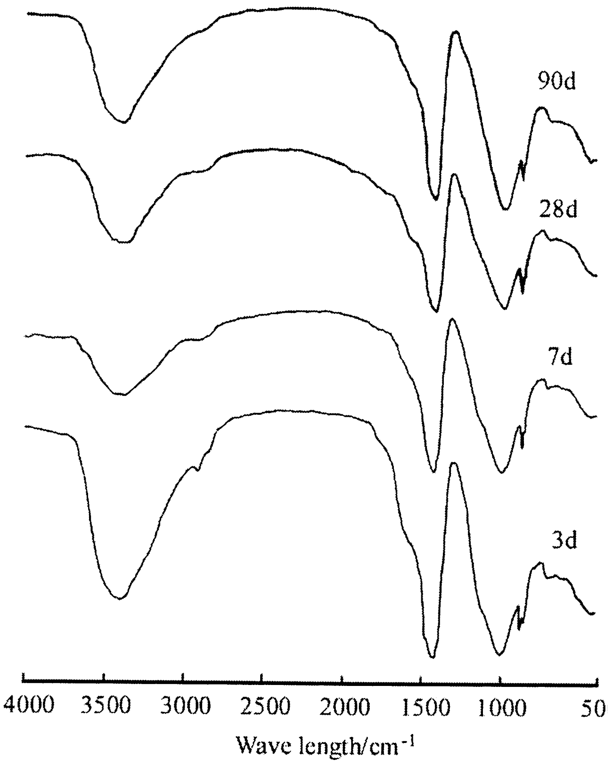

Fig. 5. IR spectra of hydrated ASRC (S1) cement paste at different curing ages.

hardened ASRC cement paste. This result is in a very good agreement with that obtained by XRD analysis.

Same TG-DTA analyses were carried out on the ambient temperature cured S2 cement paste specimen and steam-cured S1 cement paste specimen.

Table 2 listed the mass loss of the hardened ASRC cement paste specimens in four different temperature ranges, 20–200, 200–450, 450–650 and 650–950 °C, divided according to the features of thermal effect on DTA curve and the cascade feature of mass loss on TG curve during heating.

It can be seen from Table 2 that the mass loss occurred in different temperature ranges differs remarkably with different curing ages, and most of it occurs before 650 °C during heating. Mass loss occurred intensively in the temperature ranges of both 20–200 and 450–650 °C is almost in proportion to the curing age of the hardened S1 cement paste specimens.

Results of S2 specimen showing the similar DTA characteristics and the mass loss with S1 specimen were also listed in Table 3. Compared with ambient temperature cured S1 specimen, S2 shows the more total mass loss, especially more mass loss in the range of 20–200 °C but less mass loss in the range of 450–950 °C, indicating that the ambient temperature cured S2 specimen contains more free water and less chemical bonding water than those of S1 specimen.

Data listed in Table 3 also show that the hydration rate of S1 cement is significantly accelerated by treatment of steam curing. The amounts of chemically bonding water in 8, 16 and 24 h steam curing condition are almost equal to those cured at ambient temperature for 3, 7 and 90 days. Furthermore, the increase in water content in the temperature range of 450–950 °C and the decrease in the range of 20–450 °C suggests the increase of chemically bonded water or the crystalline degree of C-S-H and other hydration products in steam-cured hardened cement paste.

### 3.3. Results of IR analysis

Results of IR analysis on the ambient temperature cured hardened S1 cement paste are shown in Fig. 5. The wide absorption band at wave number 2800–3700 cm$^{-1}$ represents existence of $CaCO_3$, which shows the trend of weakening with the progress of hydration. The small absorption with two small shoulders aside at 800–1100 cm$^{-1}$ repre-

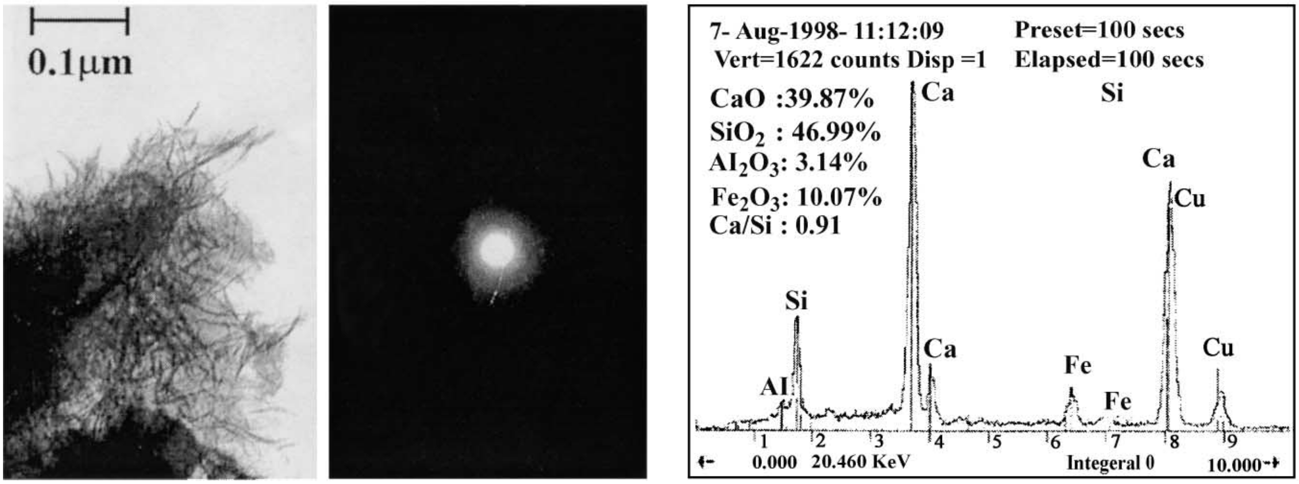

Fig. 6. TEM morphology and EDS patterns of the hydration products in hydrated ASRC (S1) cement paste.

sents existence of β-$C_2S$. The splits of the right shoulder, which can be seen in spectrum of 3-day cured specimen, disappears in spectrum of 7-day cured specimen, and the small shoulder at left side becomes smaller with the progress of hydration and vanished at 90 days, thus suggesting that β-$C_2S$ in cement decreases with the progress of hydration and contributes the hardening of the ASRC cement.

### *3.4. Results of TEM-EDXA analysis*

TEM-EDXA analysis on the morphology and chemical composition of hydration products of 90d curing age S1 cement suspension with water/cement ratio 20 are shown in Fig. 6.

Hydration products observed in the suspension specimen show aggregations made up of very small particles in fibrous shape with single particle size of about hundreds of nanometers or much smaller. The SAED analysis on these particles shows only center transparent spots, which suggests that they are amorphous materials, i.e., gel. EDS analysis on the chemical composition of these small particles reveals that they are mostly consisted of CaO and $SiO_2$ chemically, apart from some $Al_2O_3$ and $Fe_2O_3$, with their mean Ca/Si ratio 0.8–1.2. Therefore, the author believes that these amorphous materials are C-S-H gels dissolved with $Al_2O_3$ and $Fe_2O_3$ and with low Ca/Si. However, TEM observation does not find the existence of fibrous ettringite phase and crystallized calcium hydroxide.

## 4. Conclusions

1. The hydration products of ASRC cement are mostly C-S-H gel with very low Ca/Si ratio of 0.8–1.2, very small particle size of hundreds of nanometers and very irregular shape in morphology.
2. Neither crystallized calcium hydroxide and ettringite, which are normally found in hardened Portland cement paste system, nor zeolite-like phase were found in hardened ASRC cement paste system.
3. The hydration products of ASRC cement remain similar, regardless of its kind of activators, simple or composite, and curing condition, ambient temperature curing or steam curing.

## References

[1] V.D. Glukhovsky, Soil Silicates, Gosstroiizdat Publish, Kiev, USSR, 1959.

[2] J. Davidovits, Properties of geopolymer cements, Proc. of the 1st Int. Confer. Alkali. Cem. and Concr, VIPOL Stock Company, Kiev, Ukraine vol. I, (1994) 131–149.

[3] A.K. Chatterjiee, Special and new cements, Proc. of 9th Int. Congr. Chem. Cem., National Council for Cement and Building Materials (NCB), New Delhi, India vol. I, (1992) 177.

[4] J. Malolepszy, Activation of synthetic melilite slags by alkalis, Proc. of 8th Int Congr. Chem Cem, Abia Grafica e Editora Ltda. Rio de Janeiro, Brazil, vol. IV, (1986) 104.

[5] C.J. Shi, Alkali–phosphorous slag cement, J. Southeast Univ. 19 (1) (1989) 141–144.

[6] L.L. Dai, J.N. Chen, Alkali–slag–fly ash cement, Bull. Chin. Ceram. Soc. 16 (1) (1988) 25–32.

[7] R.Z. Yuan, Y. Qiong, S.X. Ouyang, Structure, hydration activity and mechanism of activation of slag, J. Wuhan Univ. Ind. Technol. 3 (1987) 297–302.

[8] X.C. Pu, C.C. Gan, L. Wu, Properties of alkali–slag cement concrete, J. Chin. Ceram. Soc. (5) (1989) 5–10.

[9] C.M. Gong, N.R. Yang, Effect of phosphate on the hydration of alkali-activated red mud–slag cementitious material, Cem. Concr. Res. 30 (7) (2000) 1013–1016.

[10] Z.H. Pan, Y. Feng, N.R. Yang, Study on solid alkali–slag–red mud cementitious material, J. Nanjing Univ. Chem. Technol. 20 (2) (1998) 34–38.

[11] Z.H. Pan, Y. Feng, N.R. Yang, Development of alkali–slag–red mud cement, J. Chin. Ceram. Soc. 18 (3) (1999) 34–39.

[12] Z.H. Pan, Alkali activated slag–red mud cementitious material, Thesis of Doctor of Engineering, Nanjing University of Chem. Tech. Nanjing, China, 1999.

[13] Z.H. Pan, Y. Feng, Y.N. Lu, N.R. Yang, Alkali–slag–red mud cement, Cem. Eng. (1) (2000) 53–56.